ELSEVIER

Catalysis Today 71 (2002) 327–334

CATALYSIS TODAY

www.elsevier.com/locate/cattod

Comparison of preparation methods for carbon nanotubes supported iron Fischer–Tropsch catalysts

Eric van Steen [a,*], Frans F. Prinsloo [a,b]

[a] *Department of Chemical Engineering, Catalysis Research Unit, University of Cape Town, Private Bag, Rondebosch 7701, South Africa*
[b] *SASTECH R&D, KlasieHavenga Road 1, Sasolburg 9586, South Africa*

Abstract

Carbon nanotubes supported iron catalysts were prepared by incipient wetness, deposition/precipitation using K_2CO_3, and deposition/precipitation using urea. The incipient wetness method and the deposition/precipitation technique using urea yielded highly dispersed Fe^{3+} on the carbon nanotubes support. The deposition/precipitation technique using K_2CO_3 also yielded larger Fe_2O_3-crystallites. After reduction the three catalysts had similar metal surface areas. Nevertheless, the activity of these catalysts in the Fischer–Tropsch synthesis differed significantly with the catalyst prepared by incipient wetness being the most active one. It is speculated that the differences in the performance of the catalysts might be attributed to the different crystallite size distributions, which would result in a variation in the amount of the different phases present in the catalyst under reaction conditions. The selectivity in the Fischer–Tropsch synthesis over the three catalysts seems to be independent of the method of preparation.

Keywords: Fischer–Tropsch synthesis; Iron; Carbon; Carbon nanotubes; Catalyst preparation

1. Introduction

Carbon materials can be used as support materials, due to their flexibility as support in tailoring the catalyst properties to specific needs [1,2]. Activated carbon has many advantages if utilised as catalyst support (resistant to acidic or basic media, stable at high temperatures in an inert atmosphere, possible to tailor its pore structure and chemical nature of the surface, etc.). Carbon nanotubes possess similar properties and in most cases outperform activated carbon in this respect [3]. The use of carbon nanotubes as support for transition metal catalysts has recently been demonstrated [3–6].

Iron catalysts supported on activated carbon have been used in the Fischer–Tropsch synthesis. It has been claimed, that they have a higher throughput per unit volume as a consequence of higher dispersions and/or metal–support interactions than unsupported iron catalysts [7], and higher olefin selectivity [7–10]. The Fischer–Tropsch synthesis over these catalysts has typically been performed at non-typical Fischer–Tropsch conditions, i.e. atmospheric pressure. Activated carbon has a micro-porous structure. Due to this structure transport limitations may occur in the reaction. This can be minimised by using carbon nanotubes, which have a predominantly meso-porous structure.

Hyperion Catalysts International patented the preparation of a carbon nanotube supported catalyst for the Fischer–Tropsch process according to the deposition precipitation method [11]. In the Fischer–Tropsch synthesis (fluidised bed reactor; $T_{rxn} = 340\,^{\circ}C$, $p = 25\,bar$, $H_2/CO = 6$) over this catalyst, an olefin selectivity of 70% in the C_5–C_{10}

* Corresponding author. Tel./fax: +27-21-650-3796.
E-mail address: evs@chemeng.uct.ac.za (E. van Steen).

0920-5861/02/$ – see front matter
PII: S0920-5861(01)00459-X

fraction and 60% in the C_{11}–C_{18} fraction was obtained. Apart from this patent the literature is scarce on the utilisation of meso-porous carbon supports in CO hydrogenation reactions at high pressures. Thus, there could be a significant incentive to investigate CO hydrogenation over carbon nanotubes supported iron catalysts at high pressure and at H_2/CO ratios closer to more practical values.

In this study, the physical characteristics of various iron-based catalysts supported carbon nanotubes are compared and their performance in the Fischer–Tropsch synthesis is compared with that of a typical Fe-based catalyst.

2. Experimental

Carbon nanotubes were obtained from the research division, SASTECH R&D, of Sasol. Prior to their use the carbon nanotubes were refluxed in nitric acid. SEM and TEM images revealed opened carbon nanotubes with a herring structure (graphite layers are arranged at an angle relative to the *z*-axis with an interlayer spacing corresponding to that of graphite). The carbon nanotubes were highly interweaved in correspondence with the so-called bird nest structure.

The catalysts were prepared according to three methods. The first method of preparation used was incipient wetness impregnation. For the preparation of this catalysts (IWCu8) 7.23 g $Fe(NO_3)_3{\cdot}9H_2O$ and 0.19 g $Cu(NO_3)_2{\cdot}3H_2O$ were dissolved into 18 cm^3 of deionised water. This mixture was added drop-wise to 10 g of the carbon nanotube support. The resulting slurry dried in a rotavaporator at 90 °C for 20 min.

In the second approach, the catalyst (DPCu) was prepared using a deposition precipitation method with potassium carbonate [12]. Ten gram of carbon nanotubes was dispersed with 600 cm^3 of deionised water for 2 min in an ultrasonic bath. This was then slurried with an additional 1 l of deionised water. One-hundred and twenty gram of a 41% iron nitrate solution was then added to the slurry. The slurry was neutralised under vigorous stirring with a solution of 20 wt.% potassium carbonate to pH > 7. The slurry was filtered, washed and subsequently dried in a vacuum oven.

In the third method, a deposition precipitation method with urea was followed (DPUCu8). For the preparation of this catalyst 7.23 g $Fe(NO_3)_3{\cdot}9H_2O$, 0.19 g $Cu(NO_3)_2{\cdot}3H_2O$, and 1.61 g urea (1.5 moles per mole of iron) were dissolved into 18 cm^3 of deionised water. This mixture was added drop-wise to 10 g of the carbon nanotube support. The resulting slurry was then subjected to heat in a rotavaporator. The water was removed by evaporation under vacuum at 90 °C for 20 min after allowing a sufficient time (at least 2 h [13]) for the hydrolyses of the urea.

After drying the catalysts in the rotavaporator all the catalysts were dried further in a vacuum oven (−800 mbar) for 2 h at 120 °C and then calcined in a nitrogen stream for 2.5 h at 220°C (flow rate = 1 dm^3(STP)/min). The resulting catalyst composition was determined using ICP-AES (Vista AZ CCD). Tables 1 and 2 show the composition of the investigated catalysts.

Table 1
Metal content of the various catalysts under investigation

Catalyst	Method of preparation	C/Fe	Fe (wt.%)	Cu (wt.%)	K (wt.%)
IWCu8	Impregnation	0.085	8.3	0.45	0
DPCu	Deposition/precipitation	0.265	25.8	1.2	4.7
DPUCu8	Deposition/precipitation with urea	0.083	8.1	0.45	0

Table 2
Metal surface area and iron crystallite size of the reduced, carbon nanotubes supported iron catalysts as obtained from H_2-chemisorption experiments

Catalyst	V_M (cm^3(STP)/g)	Metal surface area (m^2/g)	Dispersion (%)	d_{Fe} crystallite (nm)
IWCu8	2.13	6.6	3.0	9.6
DPCu	1.88	5.8	0.3	33.7
DPUCu8	2.26	7.0	3.2	8.7

The calcined catalyst precursors were characterised using XRD and Mössbauer-spectroscopy. XRD analysis was performed on a Siemens difractometer employing Ni-filtered Co Kα radiation ($\lambda = 1.7902$ Å). For the quantitative determination of the crystallite diameter the samples were grinded for 10 min in 25 cm^3 ethanol. As internal standard 5% silicon was added to the sample. The crystallite diameter $\langle L \rangle$ was determined by substituting the half-width of a chosen peak into the Debye–Scherrer equation. The value of K was taken as 0.9 for peak width at half maximum. The quantitative scanning of each sample was performed in triplicate.

Mössbauer experiments were performed with a 50 mCi (initial activity) ^{57}Co-source in a Rhodium matrix at room temperature. The spectrometer was operated in the symmetric constant acceleration mode with 100 μs of dwell time per channel. Approximately 100 mg of the sample was ground into fine powder and thereafter mixed with a Mössbauer inert material to obtain an iron mass to area ratio of ∼30 mg/cm^2 to obtain a signal with minimal distortion due to secondary effects. The data was analysed using a least-square fitting routine that models the spectra as a distribution of singlets, quadruple doublets and sextuplets based on Lorentzian line-shaped profile. The spectral components were identified based on their isomeric shift, quadruple splitting and hyperfine magnetic field. The isomeric shift values are reported relative to metallic iron (α-Fe) and the iron content of each phase was determined from their relative peak areas.

The reduction behaviour of the catalyst precursors was studied by temperature programmed reduction (TPR) using a Micromeritics TPD/TPR 2900 instrument. Ca. 0.03 g of catalyst was placed on a porous plate mounted in a $\frac{1}{4}$ in. U-shaped quartz tube. A 10% hydrogen/nitrogen mixture was introduced (flow rate = 36 cm^3(STP)/min) and the furnace was ramped from room temperature to 1173 K at 10 K/min. The H_2-concentration was monitored using a TCD.

The reduced catalysts were characterised using H_2-chemisorption. The measurements were performed on an ASAP 2010C, Micrometrics instrument. Before chemisorption measurements the sample was heated in flowing H_2 (46.6 cm^3(STP) min^{-1}) at a heating rate of 1 K/min up to 343 K followed by a heating rate of 0.5 K/min to the final reduction temperature (623 K), at which it was kept for 16 h. After reduction the catalyst was degassed for 2 h at 10^{-5} Torr at 623 K in order to eliminate the chemisorbed hydrogen. The temperature was then lowered to 20 °C below the reduction temperature while maintaining the vacuum and degassed for a further 10 min. The temperature was subsequently lowered to the 493 K to record H_2 chemisorption isotherm. Estimated crystallite sizes based on H_2 uptakes were calculated assuming spherical geometry. The stoichiometric ratio of H/Fe was assumed to be 1, and the site density 17.3 atoms/nm^2 [12].

The Fischer–Tropsch synthesis was performed in a fixed-bed micro reactor. Before the Fischer–Tropsch synthesis the catalyst was reduced in situ in hydrogen (GHSV = 1860 cm^3(STP)/(h g)) by ramping the reactor temperature at 1 K/min up to 343 K followed by a heating rate of 0.5 K/min to the final reduction temperature, at which it was kept for 16 h. After reduction the catalyst bed was cooled down to reaction temperature (493 K). The synthesis gas used for the Fischer–Tropsch synthesis had following composition: H_2: 53.6 vol.%, CO: 32.3 vol.%, CH_4: 13.0 vol.%, N_2: 0.4 vol.%, CO_2: 0.7 vol.%. The Fischer–Tropsch synthesis was performed at 25 bar with a space velocity was 1860 cm^3(STP)/(h g). In order to evaluate the mass balance argon was mixed to the pure synthesis gas as an internal standard. The ampoule technique [14] was used to withdraw samples of the feed and tail gases at 24 h intervals.

The permanent gases were separated with molecular sieve (5 Å) and Porapak Q columns and analysed using a TCD. The separation of the organic product compounds was achieved with a Petrocol DH 150 (150 m long × 0.25 mm ID coated with a 1 μm methyl silicon stationary phase film) capillary column employing a temperature program from 223 to 553 K and analysed using an FID.

3. Results and discussion

The crystallite size of the iron oxides on the carbon nanotubes support was determined from the line broadening in the X-ray diffraction patterns. Unfortunately, the crystallites in the samples prepared according to the incipient wetness method (IWCu8) and the deposition/precipitation method with urea (DPUCu8)

were too small to be quantified using this method. The unreduced catalyst sample prepared using the deposition precipitation technique (DPCu) contained mainly hematite. The peaks due to graphite ($2\theta = 30.4^\circ$ and $\sim 50.6^\circ$) were also evident from the X-ray diffraction patterns. The crystallite diameter of the hematite was estimated to be 33 ± 3 nm using the Debye–Scherrer equation.

The Mössbauer spectra of the catalyst precursors are given in Fig. 1 and the hyperfine interaction parameters obtained from the deconvolution of the spectra are given in Table 3. The Mössbauer spectra indicate the presence of small crystallites of Fe^{3+} species in all catalyst precursors. The catalyst precursor of DPCu consists of both small crystallites of Fe^{3+} containing species and large crystallites of hematite, α-Fe_2O_3, as was also shown using XRD (vide supra). The small crystallites, which gave rise to a doublet, have an average crystallite size of ca. 4 nm whereas the large crystallites have an average diameter of ca. 12 nm. The Fe^{3+}-species, which have large quadrupole moments, are in a highly asymmetric environment for Fe^{3+}. This might be ascribed to a well-dispersed layer of iron oxide, or oxyhydroxide on the surface of the carbon nanotube support. The Fe^{3+} species, which have small quadrupole moments, are due to Fe^{3+} atoms located in the bulk of the material.

The reduction behaviour of the calcined catalyst precursors was studied using TPR (see Fig. 2). The total amount of hydrogen consumed during TPR is given in Table 4 (the amount of hydrogen used for the reduction of CuO to Cu has been corrected for). For complete reduction of trivalent iron a molar ratio of H_2/Fe of 1.5 should be obtained. The presence of car-

Table 3
Hyperfine parameters obtained from the Mössbauer spectra of the calcined precursors of the iron catalysts supported on carbon nanotubes

Catalyst	δ (mm s^{-1})	ΔE_Q (mm s^{-1})	Phase	Phase ratio
IWCu8	0.36	1.02	Fe^{3+}	33.0
	0.36	0.65	Fe^{3+}	67.0
DPCu	0.38	−0.26	α-Fe_2O_3	17.5
	0.34	1.08	Fe^{3+}	27.8
	0.34	0.62	Fe^{3+}	54.7
DPUCu8	0.32	1.12	Fe^{3+}	34.4
	0.34	0.61	Fe^{3+}	65.6

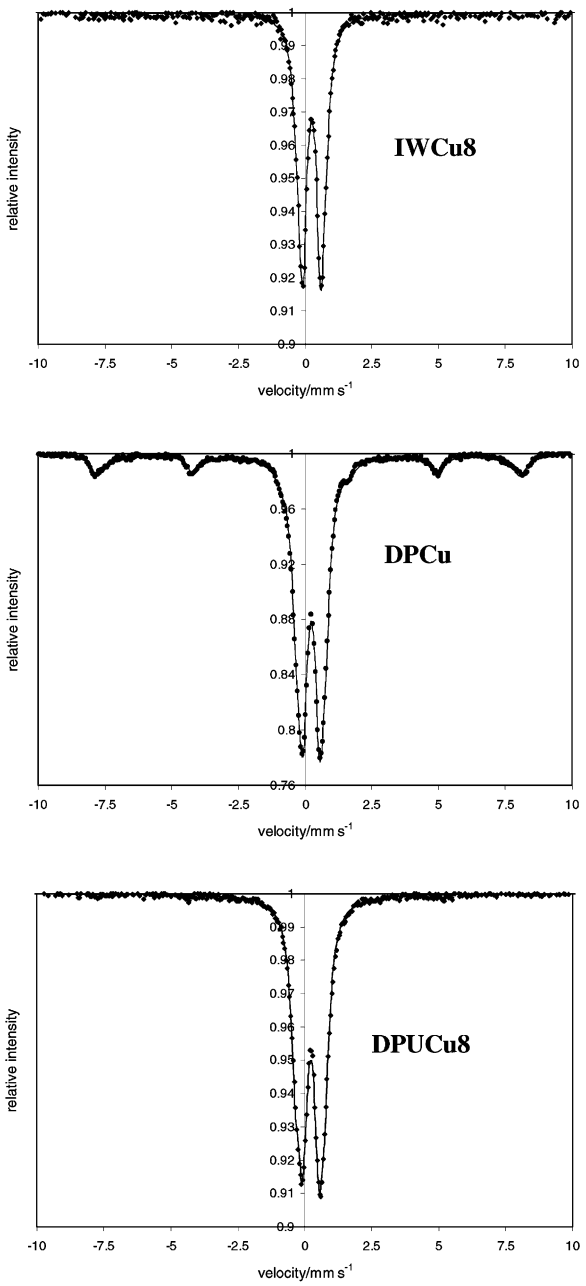

Fig. 1. Mössbauer spectra of calcined catalyst precursors (prepared using incipient wetness (IWCu8), deposition/precipitation with K_2CO_3 (DPCu) and deposition/precipitation with urea (DPUCu8)).

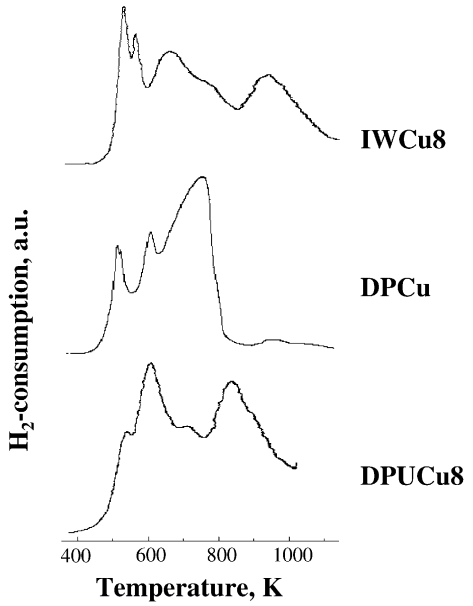

Fig. 2. TPR profiles of calcined catalyst precursors (prepared using incipient wetness (IWCu8), deposition/precipitation with K_2CO_3 (DPCu) and deposition/precipitation with urea (DPUCu8)) ($m_{catalyst} = 0.03$ g; reducing gas: 10% H_2 in N_2; flow rate = 36 cm^3(STP) min^{-1}: heating rate: 10 K min^{-1}).

bon nanotubes support may enhance H_2-consumption, since supported transition metal acts as catalyst for the formation of methane via a reaction of hydrogen with the carbon nanotubes support at high temperatures larger than 800 K. This was confirmed by measuring the methane concentration as a function of temperature in a separate experiment. The hydrogen consumption per mole of Fe is, however, much lower than the minimum required ratio (1.5) for complete reduction. This shows that a very low the degree of reduction was obtained, despite the high temperature in the TPR-experiment. Especially, the catalyst prepared using the deposition/precipitation with K_2CO_3 (DPUCu) is difficult to reduce. This might be ascribed to iron present within the nanotubes, which might be blocked by other metal crystallites. Hence, the iron within the nanotubes is no longer assessable for hydrogen [15].

Table 4
Hydrogen consumption during TPR calcined precursors of the iron catalysts supported on carbon nanotubes (H_2-consumption for the reduction of CuO to Cu has been subtracted from total H_2-consumption)

Catalyst	Amount of H_2 consumed (mol H_2/mol Fe)
IWCu8	1.08
DPCu	0.51
DPUCu8	1.35

The spectra are characterised by multiple peaks indicative of multiple processes taking place. The individual peaks are not well resolved. The high temperature peak in the TPR-spectra of IWCu8 and DPUCu8 can be attributed partially to the gasification of the carbon nanotubes support. This peak is absent in the TPR-spectrum of the catalyst prepared by deposition/precipitation using K_2CO_3. It might be speculated, that with this catalyst the support is not in intimate contact with the freshly reduced metal particles.

The metal crystallite size and the metal surface area of the reduced catalyst was determined using H_2-chemisorption (see Table 2). These measurements were performed at rather elevated temperature (493 K), since the chemisorption of hydrogen is activated and high temperatures are required for high coverage on small supported iron crystallites [8,9,16] and unsupported iron crystallites [17]. The metal surface areas of the catalysts prepared using the three different methods are comparable ($6.5 \pm 0.5\,m^2/g$). The preparation of the catalysts using incipient wetness technique (IWCu8) and using the deposition/precipitation technique with urea (DPCu8) yielded approximately the same crystallite size (9.6 and 8.7 nm, respectively). The preparation of the catalyst using the deposition/precipitation with potassium carbonate yielded much larger crystallite size. The obtained size is comparable to that of the hematite in the calcined catalyst (as determined using XRD—vide supra). This indicates some sintering using the reduction procedure applied, since upon reduction of hematite a decrease of 23% in the diameter of spherical crystallites can be expected.

The performance of the carbon nanotubes supported iron based catalysts in the Fischer–Tropsch synthesis was tested in a fixed bed reactor. The time-on-stream behaviour of these catalysts is demonstrated in Fig. 3 and Table 5. The initial activity of the catalyst prepared by the incipient wetness technique (IWCu8) was initially high, but declined significantly with time on stream. The activity of the catalysts prepared by deposition/precipitation (DPCu

and DPUCu8) was much lower. This is a surprising observation, since the metal surface area of these catalysts is comparable. It was expected that the catalyst prepared by the deposition/precipitation method with K_2CO_3 (DPCu) might have a higher activity, since it contained significant amount of potassium, which is a promoter for iron based Fischer–Tropsch catalysts. It is, however, not clear whether potassium is associated with iron or with residual acidic sites on the carbon nanotubes. The metal crystallite size, as determined by H_2-chemisorption, for the catalysts prepared by incipient wetness (IWCu8) and deposition/precipitation with urea (DPUCu8), were quite similar. Nevertheless, the behaviour of these catalysts in the Fischer–Tropsch synthesis is completely different. It might be speculated that the origin of the difference in the activity is related to the difference in the metal crystallite size distribution in these catalysts, which would result in a different extent of the phases present in the active Fischer–Tropsch catalyst.

The CO_2-yield obtained with these catalysts is moderate (see Fig. 3). A high CO_2-selectivity (45% C) was obtained initially with the catalyst prepared by the deposition/precipitation method with K_2CO_3 (DPCu). After 96 h on stream the CO_2-selectivity is for all catalysts rather low (10–20% C). The addition of potassium to iron based Fischer–Tropsch catalysts is known to enhance carbon deposition [18], and hence an initially higher CO_2-yield can be expected for K-promoted iron catalysts.

The chain growth probability is comparable to that what is usually obtained with iron-based catalysts under similar conditions. The slight differences are most

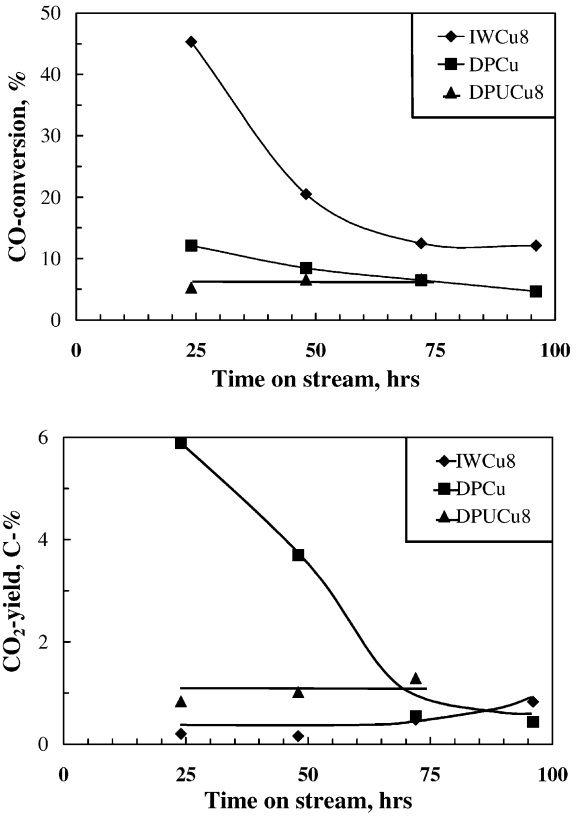

Fig. 3. Time on stream behaviour of the Fischer–Tropsch synthesis over the iron catalysts supported on carbon nanotubes ($T_{reduction}$ = 493 K; $t_{reduction}$ = 4 h; reduction gas: H_2; GHSV = 1860 cm^3(STP)/(g h); $T_{reaction}$ = 493 K; $p_{reaction}$ = 25 bar; synthesis gas: 53.6% H_2, 32.3% CO; GHSV = 1860 cm^3(STP)/(g h)). (Top): CO-conversion as a function of time on stream. (Bottom): CO_2-yield as a function of time on stream.

Table 5
Activity and selectivity in the Fischer–Tropsch synthesis over the iron catalysts supported on carbon nanotubes after 24 h on stream and in brackets after 96 h on stream ($T_{reduction}$ = 493 K; $t_{reduction}$ = 4 h; reduction gas: H_2; GHSV = 1860 cm^3(STP)/(g h); $T_{reaction}$ = 493 K; $p_{reaction}$ = 25 bar; synthesis gas: 53.6% H_2, 32.3% CO; GHSV = 1860 cm^3(STP)/(g h))

Catalyst	X_{CO} (%)	Activity		Y_{CO_2} (%C)	S_{CO_2} (%C)	α_1[a]	α_2[b]
		mmol/(g h)[c]	mmol/(m^2 h)[d]				
IWCu8	45.3	12.1 (3.3)	1.8 (0.5)	0.2 (0.8)	0.4 (6.9)	0.64	–
DPCu	12.1	3.3 (1.2)	0.6 (0.2)	5.9 (0.4)	48.7 (9.5)	0.67	0.83
DPUCu8	3.62	1.0 (1.8)	0.2 (0.3)	0.7 (1.3)	16.0 (19.5)	0.67	0.83

[a] CO consumption per gram of catalyst and hour.
[b] CO consumption per metre square of metal surface area (as determined by H_2-chemisorption) and hour.
[c] Chain growth probability in the range of C_3–C_6.
[d] Chain growth probability in the range of C_8–C_{13}.

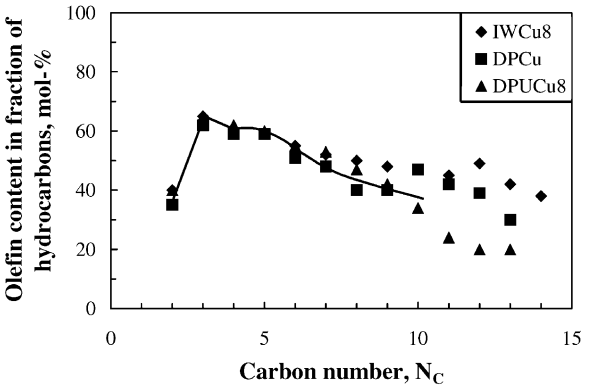

Fig. 4. Olefin content oin the fraction of hydrocarbons as a function of carbon number in the Fischer–Tropsch synthesis over the iron catalysts supported on carbon nanotubes ($T_{reduction} = 493\,K$; $t_{reduction} = 4\,h$; reduction gas: H_2; GHSV $= 1860\,cm^3(STP)/(g\,h)$; $T_{reaction} = 493\,K$; $p_{reaction} = 25\,bar$; synthesis gas: 53.6% H_2, 32.3% CO; GHSV $= 1860\,cm^3(STP)/(g\,h)$; time on stream; 96 h).

likely due to the different conversion levels over this catalyst [19]. The different preparation methods do not seem to affect the selectivity of the Fischer–Tropsch synthesis significantly. The methane selectivity also seems to be in the range of what is usually reported for iron based catalysts under similar reaction conditions (methane selectivity is not shown here; due to the large methane content of the synthesis gas the exact methane selectivity determination is associated with large errors).

It has been claimed that the Fischer–Tropsch synthesis over carbon nanotubes supported iron catalysts yields more olefins [7–11]. Fig. 4 shows the olefin content in the fraction of linear hydrocarbons after 96 h on stream. The olefin selectivity does not differ much between the catalysts prepared according to the various methods. The scatter, especially at high carbon number, can be attributed to the difference in the reaction conditions, i.e. the difference in the CO-conversion.

4. Conclusions

Carbon nanotubes supported iron catalysts were prepared using three different methods, viz. incipient wetness, deposition/precipitation using K_2CO_3, and deposition/precipitation using urea. The iron catalyst was promoted with copper (Cu/Fe = 0.04–0.05 mol/mol). The catalyst prepared by the deposition/precipitation method with K_2CO_3 also contained potassium, which is known to be a promoter for the iron-based Fischer–Tropsch catalysts. The incipient wetness method and the deposition/precipitation technique using urea yielded highly dispersed Fe^{3+} on the carbon nanotubes support. The deposition/precipitation technique using K_2CO_3 yielded larger Fe_2O_3-crystallites, besides highly dispersed Fe^{3+}. After reduction all three catalysts had similar metal surface areas. Nevertheless, the activity of these catalysts in the Fischer–Tropsch synthesis differed significantly. The catalyst prepared by incipient wetness was the most active, although its activity declined strongly with time on stream. It is speculated that the differences in the activity of the catalysts might be attributed to the different crystallite size distributions, which would result in a variation in the amount of the different phases present in the catalyst under reaction conditions. The selectivity in the Fischer–Tropsch synthesis over the three catalysts seems to be independent of the method of preparation.

Acknowledgements

Financial support for this project from Sasol is greatly acknowledged.

References

[1] H. Marsh, E.A. Heintz, F. Rodriquez-Reinoso, Introduction to Carbon Technologies, Alicante, 1997.
[2] F. Rodriquez-Reinoso, Carbon 36 (1998) 159.
[3] N.M. Rodriguez, M.-S. Kim, R.T. Baker, J. Phys. Chem. 98 (1994) 13108.
[4] M.S. Hoogenraad, R.A.G.M.M. Van Leeuwarden, G.J.B. van Breda-Vriesman, A. Broersma, A.J. Van Dillen, J.W. Geus, in: G. Poncelet, J. Martens, B. Delmon, P.A. Jacobs, P. Grange (Eds.), Metal Catalysts Supported on a Novel Carbon Support, Elsevie, Amsterdam, 1995.
[5] J.M. Planeix, N. Coustel, B. Coq, V. Brotons, P.S. Kunbhar, R. Dutartre, P. Geneste, P. Bernier, P.M. Ajayan, J. Am. Chem. Soc. 116 (1994) 7935.
[6] M.S. Hoogenraad, M.F. Onwezen, A.J. Van Dillen, J.W. Geus, Stud. Surf. Sci. Catal. 103 (1996) 719.
[7] H.-J. Jung, P.L. Walker Jr., M.A. Vannice, J. Catal. 75 (1982) 416.
[8] H.-J. Jung, M.A. Vannice, L.N. Mulay, R.M. Stanfield, W.N. Delgass, J. Catal. 76 (1982) 208.

[9] A.P.B. Sommen, F. Stoop, K. van Der Wiele, Appl. Catal. 14 (1985) 277.
[10] A.A. Chen, M.A. Vannice, J. Phillips, J. Phys. Chem. 91 (1987) 6257.
[11] V.K. Jones, L.R. Neubauer, C.H. Bartholomew, J. Phys. Chem. 90 (1986) 4832.
[12] D. Moy, US Patent, WO 93/24214 (1992).
[13] K. De Jong, A.J. van Dillen, Heterogeneous Catalysis: Preparation, Characterisation and Application, Publicard, 1999.
[14] H. Schulz, A. Geertsema, Erdöl und Kohle 30 (1977) 93.
[15] S.C. Tsang, Y.K. Chen, R.M. Lago, M.L.H. Green, Open carbon nanotubes as novel supports in heterogeneous catalysis, in: H. Kuzmany (Ed.), Fullerenes Fullerene Nanostructers, Proc. 10th Int. Wintersch. Electron. Prop. Novel Mater, World Scientific, Singapore, 1996.
[16] R. Reuel, C. Bartholomew, J. Catal. 85 (1984) 63.
[17] P.H. Emmett, R.W. Harkness, J. Am. Chem. Soc. 57 (1935) 1961.
[18] H. Schulz, Erdöl und Kohle 30 (1977) 123.
[19] H. Schulz, E. van Steen, M. Claeys, Stud. Surf. Sci. Catal. 81 (1994) 455.